

## ARTICLE

## Kartogenin induces cartilage-like tissue formation in tendon–bone junction

Jianying Zhang and James H-C Wang

**Tendon–bone junctions (TBJs) are frequently injured, especially in athletic settings. Healing of TBJ injuries is slow and is often repaired with scar tissue formation that compromises normal function. This study explored the feasibility of using kartogenin (KGN), a biocompound, to enhance the healing of injured TBJs. We first determined the effects of KGN on the proliferation and chondrogenic differentiation of rabbit bone marrow stromal cells (BMSCs) and patellar tendon stem/progenitor cells (PTSCs) *in vitro*. KGN enhanced cell proliferation in both cell types in a concentration-dependent manner and induced chondrogenic differentiation of stem cells, as demonstrated by high expression levels of chondrogenic markers aggrecan, collagen II and Sox-9. Besides, KGN induced the formation of cartilage-like tissues in cell cultures, as observed through the staining of abundant proteoglycans, collagen II and osteocalcin. When injected into intact rat patellar tendons *in vivo*, KGN induced cartilage-like tissue formation in the injected area. Similarly, when KGN was injected into experimentally injured rat Achilles TBJs, wound healing in the TBJs was enhanced, as evidenced by the formation of extensive cartilage-like tissues. These results suggest that KGN may be used as an effective cell-free clinical therapy to enhance the healing of injured TBJs.**

*Bone Research* (2014) 2, 14008; doi:10.1038/boneres.2014.8; Published online 13 May 2014

## INTRODUCTION

Tendons connect muscles to bones through tendon–bone junctions (TBJs), which are also referred to as entheses, insertion sites, or osteotendinous junctions.<sup>1</sup> TBJs are unique structures made of tendon, a transitional fibrocartilage zone (uncalcified and calcified) and bone.<sup>2–3</sup> The fibrocartilage structure acts as a shock absorber and reduces stress transmitted to tendons.<sup>4</sup> However, because tendons allow complex movements in multiple axes, the TBJs experience high levels of stress, making them prone to acute or chronic injuries,<sup>1</sup> particularly for those participating in recreational and highly-competitive sport activities.

Once TBJs are injured, natural healing of the injured TBJ is extremely slow, primarily because healing takes place between two different types of tissues, i.e., tendon and bone.<sup>5</sup> Even when healed, the fibrocartilage zone is not completely regenerated, making it susceptible to re-injury.<sup>6–8</sup> Previous studies have shown that the transitional fibrocartilage zone does not regenerate in human supraspinatus reattachment,<sup>9</sup> infraspinatus reattachment<sup>10</sup> or a rabbit partial patellectomy repair model.<sup>6,8,11</sup> Treatments

for these injuries almost always involve reattachment of the bone to the injured tendon by surgical juxtaposition of tendons and bones, such as in Achilles tendon and in anterior cruciate ligament (ACL) reconstruction, where a tendon graft is inserted in the bone tunnel to support tendon/bone interface healing. The outcome of ACL reconstruction largely depends on the healing of the tendon graft–bone tunnel. Unfortunately, all four zones in the injured TBJ are often not completely restored after healing, resulting in lower interface healing quality. Indeed, magnetic resonance imaging (MRI) and biopsy evaluations of human patients have shown the absence of fibrocartilage zone regeneration even several years after ACL reconstruction.<sup>7</sup> These studies emphasize that neither natural healing nor surgical interventions are sufficient to optimally restore the unique features of the fibrocartilage transition zone in injured TBJs.

Previous studies have shown the ability of tissue engineering (TE) approaches to accelerate regeneration of the tendon/bone interface. These include the use of growth factors,<sup>12–17</sup> mesenchymal stem cells (MSCs)<sup>18–19</sup> and

periosteal graft augmentation.<sup>20–22</sup> Besides these TE methods, the use of osteogenic matrix cell sheets (OMCS) has enhanced early tendon-to-bone tunnel healing. Indeed, macrophage depletion after ACL reconstruction has been shown to promote healing at the tendon/bone interface<sup>23</sup> and transplantation of OMCS with grafted tendons in rabbits induced bone formation.<sup>24</sup> In addition, implantation of a bovine-derived bone tissue scaffold into a sheep rotor cuff model also enhanced regeneration of the tendon/bone interface. In particular, all four fibrocartilage zones at the interface were regenerated, resulting in a healed interface that was similar to the normal tendon/bone interface structure.<sup>25</sup> Although these methods have shown promise in enhancing tendon graft-bone healing in animal models, at least some have inherent limitations, particularly from a clinical perspective. For example, the use of exogenous growth factors may raise safety concerns, and the use of MSCs, OMCSs or tissue scaffolds in clinical settings may not be feasible because many clinics lack the equipment and personnel to perform stem cell isolation, culture or expansion, or to create the tissue scaffold itself. Finally, periosteal grafts have been shown to cause morbidity in the autograft harvest sites.<sup>26</sup> Therefore, novel approaches are still needed to augment and accelerate TBJ healing.

Recently, a small heterocyclic molecule called kartogenin (KGN) was demonstrated to promote robust chondrocyte differentiation of primary human MSCs.<sup>27</sup> KGN induced human MSCs to express a typical set of chondrogenic genes, form chondrocyte nodules, and exhibit characteristic chondrocyte functions. These chondrocytes proliferated quickly and produced a cartilage matrix. When KGN was injected intra-articularly into a mouse model of osteoarthritis, regeneration of the cartilage was observed within only a few weeks. However, thus far KGN has not been used to promote healing of injured TBJs. Therefore, in this study we hypothesized that KGN injections would enhance the healing of injured TBJs. To test this hypothesis, we performed *in vitro* experiments using cell culture models by applying KGN to two types of adult stem cells which are involved in the healing of TBJs: bone marrow stromal cells (BMSCs) and tendon stem/progenitor cells. In addition, we also injected KGN into intact patellar tendons and experimentally injured rat Achilles tendons as *in vivo* models to investigate whether KGN could induce chondrogenesis in these tissues. Our results showed that KGN induced chondrogenesis *in vitro* and promoted the formation of cartilage-like tissues *in vivo*.

## MATERIALS AND METHODS

BMSC and patellar tendon stem/progenitor cells (PTSC) isolation and culture

BMSCs were obtained from femur bones and PTSCs were isolated from patellar tendons of seven New Zealand white

rabbits (4–6 months old females) based on protocols similar to those described previously.<sup>28–29</sup> The protocols for using rabbits in this study were approved by the University of Pittsburgh IACUC. Briefly, BMSCs isolated from the femoral marrow compartments were cultured in Dulbecco's modified Eagle's medium (Lonza, Walkersville, MD, USA) supplemented with 20% fetal bovine serum (Atlanta Biologicals, Lawrenceville, GA, USA), 100 U·mL<sup>-1</sup> penicillin and 100 µg·mL<sup>-1</sup> streptomycin (Atlanta Biologicals, Lawrenceville, GA, USA) in an incubator at 37 °C with 5% CO<sub>2</sub>. After an overnight culture, non-adherent cells were removed carefully and replaced with fresh medium. When primary cultures became almost confluent, cells were treated with 0.25% trypsin containing 0.02% ethylenediaminetetraacetic acid for 2 min at room temperature (21 °C) and seeded into new culture flasks. A pure population of BMSCs was obtained 3 weeks after the first culture was initiated. For PTSC isolation, tendon sheaths from the patellar tendons were removed to obtain the core portions of the tendons. Tendon samples were then minced into small pieces and each 100 mg wet tissue sample was digested in 1 mL phosphate buffered saline (PBS) containing 3 mg collagenase type I and 4 mg dispase at 37 °C for 1 h. After centrifugation at 3 500 r·min<sup>-1</sup> for 15 min to remove the enzymes, the cells were cultured in growth medium supplemented with 100 µmol·L<sup>-1</sup> 2-mercaptoethanol (Sigma-Aldrich, St Louis, MO, USA) at 37 °C with 5% CO<sub>2</sub>. The medium was changed every 3 days and cells were split when >90% confluence was reached. In all further culture experiments, BMSCs and PTSCs at passage 1 or 2 were used.

### *In vitro* experiments

Rabbit BMSCs or PTSCs at passage 1–2 were seeded in 6-well plates at a density of  $6 \times 10^4$  per well and cultured for two weeks in growth medium (Dulbecco's modified Eagle's medium plus 20% fetal bovine serum) with various concentrations (1 nmol·L<sup>-1</sup>–5 µmol·L<sup>-1</sup>) of KGN. The medium was changed every 3 days and after 2 weeks, cell proliferation was measured by population doubling time (PDT), and cell differentiation was assessed by measuring the expression of chondrogenic markers (aggrecan, collagen type II and Sox-9) using quantitative RT-PCR (qRT-PCR), cytochemical and immunocytochemical staining for proteoglycans, collagen type II and osteocalcin.

Determination of PDT for measuring cell proliferation *in vitro*

Proliferation of KGN treated BMSCs and PTSCs was determined by the time taken for the cells to multiply and was expressed as PDT, which was calculated from the formula  $PDT = \log_2 [N_c/N_0]$ , where  $N_0$  is the total number of cells seeded initially and  $N_c$  is the total number of cells at confluence.<sup>29</sup>

**Table 1.** Sequences of the primers used in qRT-PCR

Gene	Primer sequence	Reference
Aggrecan	Forward 5'-GAG GAG ATG GAG GGT GAG GTC TT-3'	[31]
	Reverse 5'-CTT CGC CTG TGT AGC AGA ATG-3'	
Collagen II	Forward 5'-TGG GTG TTC TAT TTA TTT ATT GTC TTC CT-3'	[30]
	Reverse 5'-GCG TTG GAC TCA CAC CAG TTA GT-3'	
Sox-9	Forward 5'-AGT ACC CGC ACC TGC ACA AC-3'	[30]
	Reverse 5'-CGC TTC TCG CTC TCG TTC AG-3'	
GAPDH	Forward 5'-ACT TTG TGA AGC TCA TTT CCT GGT-3'	[30]
	Reverse 5'-GTG GTT TGA GGG CTC TTA CTC CTT-3'	

Gene expression analysis in BMSCs and PTSCs by qRT-PCR. Total RNA (1 µg), which was extracted from BMSCs and PTSCs in each group using the RNeasy Mini Kit (Qiagen, Valencia, CA, USA), was used to synthesize first-strand cDNA by reverse transcription using SuperScript II (Invitrogen, Grand Island, NY, USA). The incubation temperatures for the cDNA synthesis started with 65 °C for 5 min followed by cooling at 4 °C for 1 min, reverse transcription at 42 °C for 50 min and a final incubation at 72 °C for 15 min. Then, qRT-PCR was performed using the Qiagen QuantiTect SYBR Green PCR Kit (Qiagen) in a 25 µL PCR reaction volume with 2 µL cDNA (total 100 ng RNA) in a Chromo 4 Detector (MJ Research, St Bruno, Que., Canada). PCR cycling conditions consisted of an initial denaturation at 94 °C for 5 min, followed by 30–40 cycles of 1 min at 94 °C, 40 s at 57 °C, 50 s at 72 °C and a final 10 min extension at 70 °C. Rabbit-specific primers for aggrecan, collagen type II, and Sox-9, and the internal control glyceraldehyde 3-phosphate dehydrogenase (GAPDH), were adopted from a previous study.<sup>30–31</sup> All primers were synthesized by Invitrogen and are listed in Table 1. Expression of all genes was normalized to the control group without KGN treatment. Relative expression levels of individual genes were calculated using the  $2^{-\Delta\Delta C_T}$  method, where  $\Delta\Delta C_T = (C_{T_{\text{target}}} - C_{T_{\text{GAPDH}}})_{\text{treated}} - (C_{T_{\text{target}}} - C_{T_{\text{GAPDH}}})_{\text{control}}$  and  $C_T$  represents the threshold cycle of each cDNA sample. At least three  $C_T$  values were used to determine the mean ± standard deviation (s.d.) for each data set.

#### Cytochemical staining of BMSCs and PTSCs *in vitro*

To determine the effect of KGN on rabbit BMSC and PTSC differentiation, cells at passage 2 were seeded into 6-well plates at a density of  $24 \times 10^4$  per well and treated with various concentrations of KGN. After two weeks of treatment, the cells were fixed with cold ethanol and stained within the culture plate wells with Safranin O or Alcian blue using standard protocols<sup>32</sup> to detect proteoglycans and collagens, respectively.

#### Immunocytochemical staining of BMSCs and PTSCs treated with KGN

To determine the influence of KGN on rabbit BMSC and PTSC differentiation, cells at passage 2 were seeded into

12-well plates at a density of  $3 \times 10^4$  per well and treated with various concentrations ( $1 \text{ nmol} \cdot \text{L}^{-1}$ – $5 \text{ } \mu\text{mol} \cdot \text{L}^{-1}$ ) of KGN. After 2 weeks of treatment, cells from each group were fixed in 4% paraformaldehyde in PBS at room temperature for 30 min. Then, chondrogenesis in the cells was determined by measuring collagen type II expression after immunostaining with mouse anti-collagen II (1:300) primary antibody (Cat. #CP18–100UG; Millipore, Billerica, MA), and osteogenesis expression was assessed using mouse anti-osteocalcin (1:300) monoclonal antibody at room temperature for 2 h (Cat. #ab13418; Abcam, Cambridge, MA). After washing in PBS three times, the proteins were detected by incubation with FITC-conjugated goat anti-mouse IgG (1:500) for collagen type II and Cy3-conjugated goat anti-mouse IgG (1:500) for osteocalcin at room temperature for 2 h. After removing unbound antibodies by washing in PBS, the nuclei were stained with Hoechst fluorochrome 33342. Finally, positively stained cells were examined under fluorescence microscopy (Nikon eclipse microscope, TE2000-U, Nikon Instruments Inc., Melville, NY, USA).

#### *In vivo* injection experiments

For *in vivo* injection experiments, 12 female Sprague–Dawley rats (2.5–3.5 months old) were used. The protocol for using rats in our *in vivo* experiments was approved by the University of Pittsburgh IACUC. Two models were used to determine the effect of KGN injections *in vivo*. In the first model, a wound with 1 mm diameter was created in the Achilles TBJs in both hind legs of all 12 rats using a biopsy punch (Miltex Inc., York, PA, USA). Then rats were divided into two groups based on the injections received: six rats were given 10 µL saline injections in each wound (wound-only group) and six rats received 10 µL of  $100 \text{ } \mu\text{mol} \cdot \text{L}^{-1}$  KGN solution each in the wounded areas (wound+KGN group). The injections were given immediately after wounding and repeated on days 2, 4, 7 and 12. The KGN dosage used in the injection experiments was based on a previous study.<sup>27</sup> After injections, all rats were allowed free cage activities. In the second model, the intact patellar tendons in the hind legs of the wound only group received 10 µL saline, while each intact patellar tendon in the wound+KGN group received 10 µL of  $100 \text{ } \mu\text{mol} \cdot \text{L}^{-1}$  KGN solution. Then they were all killed on day 15 post-treatment to harvest the Achilles TBJs ( $n=12$ ; two from each of the six rats) and the patellar tendons ( $n=12$ ; two from each of the six rats). After morphological examination of the wounded area, cartilage formation in each TBJ was determined by immunostaining of frozen tissue sections.

For immunohistochemical analyses, both patellar and Achilles tissues were immersed in frozen section medium (Neg 50; Richard-Allan Scientific; Kalamazoo, MI, USA) in pre-labeled base molds and quickly frozen by placing in 2-methylbutane chilled in liquid nitrogen. The frozen tissue

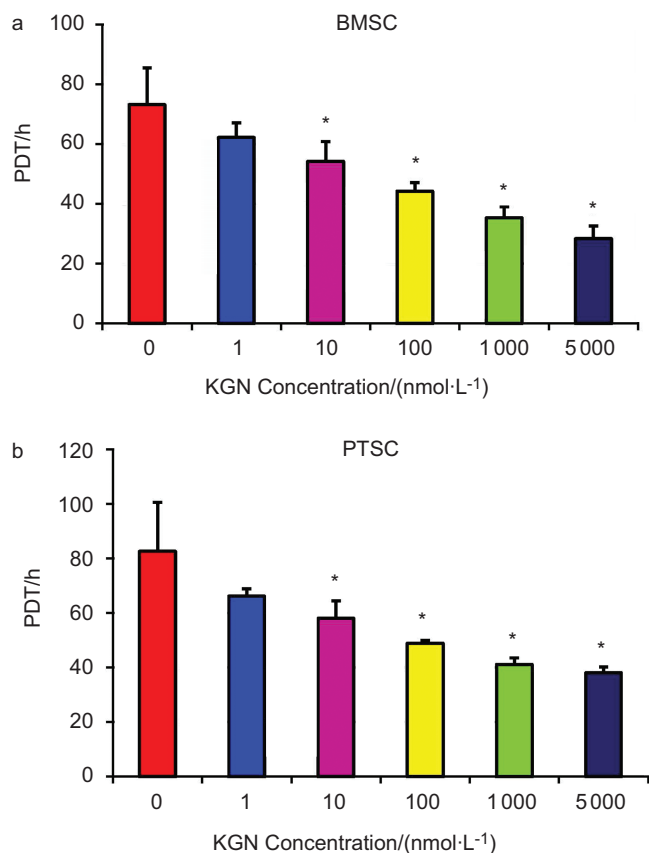


**Figure 1.** The effect of KGN on the proliferation of rabbit BMSC (a) and PTSCs (b) *in vitro*. BMSCs and PTSCs were cultured with various concentrations of KGN ( $1 \text{ nmol}\cdot\text{L}^{-1}$ – $5 \mu\text{mol}\cdot\text{L}^{-1}$ ) for 3 days. Cell proliferation in both cultures was assessed by determining cell PDT. Increasing KGN concentrations decreased PDT in both BMSCs and PTSCs, indicating higher cell proliferation rates in response to KGN treatments. The data are expressed as mean  $\pm$  s.d. of three independent experiments. Asterisks represent significant differences ( $P < 0.05$ ) between the treatment groups with various KGN concentrations and the control group, or the cells without KGN treatment.

blocks were then placed on dry ice and subsequently stored at  $-80^\circ\text{C}$  until further use.

Histochemical analysis of tissues treated *in vivo* with KGN. Each frozen tissue block was cut into  $8 \mu\text{m}$ -thick sections, which were fixed in 4% paraformaldehyde for 15 min. For histochemical staining, the tissue sections ( $8 \mu\text{m}$  thick) were stained with Safranin O and fast green according to standard protocols to detect proteoglycan and collagen expression, respectively.<sup>32</sup>

#### Statistical analysis

Data are expressed as mean  $\pm$  standard deviation (mean  $\pm$  s.d.) of three independent experiments, each with at least three replicates. A two-tailed Student's *t*-test was used for statistical analysis. A *P*-value less than 0.05 was considered to indicate a significant difference between each KGN treated group and its control group.

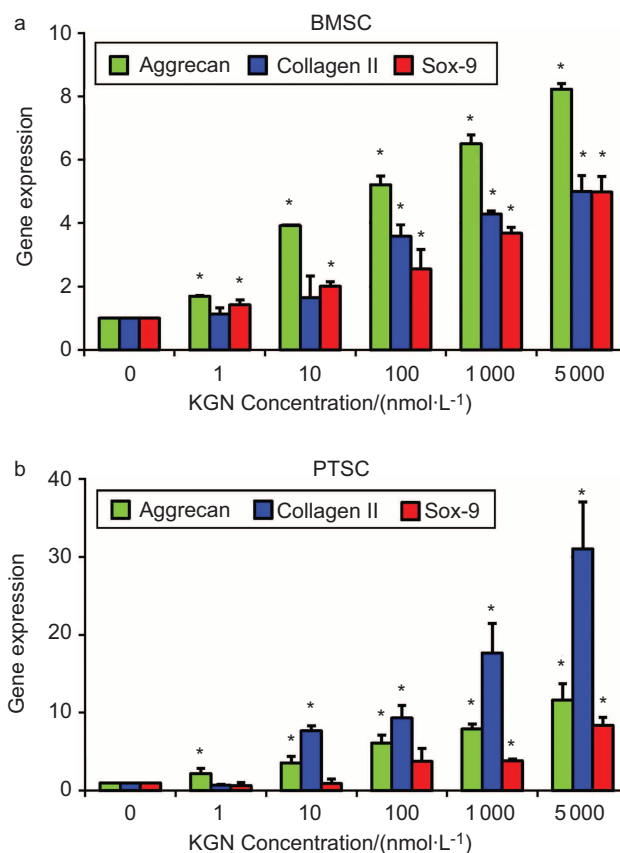


**Figure 2.** The effect of KGN on the gene expression of rabbit BMSC (a) and PTSC (b) *in vitro*. Rabbit BMSCs and PTSCs were grown in medium containing KGN at concentrations ranging from  $1 \text{ nmol}\cdot\text{L}^{-1}$  to  $5 \mu\text{mol}\cdot\text{L}^{-1}$  for 7 days, followed by RNA extraction and qRT-PCR to determine expression levels of chondrogenesis markers aggrecan, collagen II and Sox-9. In both cell types, KGN increased the expression of all three genes in a dose-dependent manner. Data represent mean  $\pm$  s.d. of three independent experiments. Asterisks indicate significant statistical differences ( $P < 0.05$ ) between the different KGN treatments and their respective controls ( $0 \text{ nmol}\cdot\text{L}^{-1}$  KGN).

## RESULTS

### Effects of KGN on BMSCs and PTSCs *in vitro*

Proliferation of BMSCs and PTSCs treated with various concentrations of KGN in culture increased significantly, as revealed by a reduction in PDT (Figure 1). KGN significantly decreased PDT in both cell types in a concentration-dependent manner, with BMSCs reaching the lowest PDT at a KGN concentration of  $5 \mu\text{mol}\cdot\text{L}^{-1}$  (Figure 1). Similarly, PTSCs proliferated more quickly when the KGN concentration was gradually raised from  $1 \text{ nmol}\cdot\text{L}^{-1}$  to  $5 \mu\text{mol}\cdot\text{L}^{-1}$ .

Expression levels of all three chondrogenic genes, aggrecan, collagen type II (collagen II), and Sox-9, were highly elevated in both BMSCs and PTSCs treated with KGN (Figure 2) compared to control cells without KGN treatment. In BMSCs, significant increase was observed in the expression levels of aggrecan and Sox-9 even at the lowest KGN concentration ( $1 \text{ nmol}\cdot\text{L}^{-1}$ ) and these levels rose

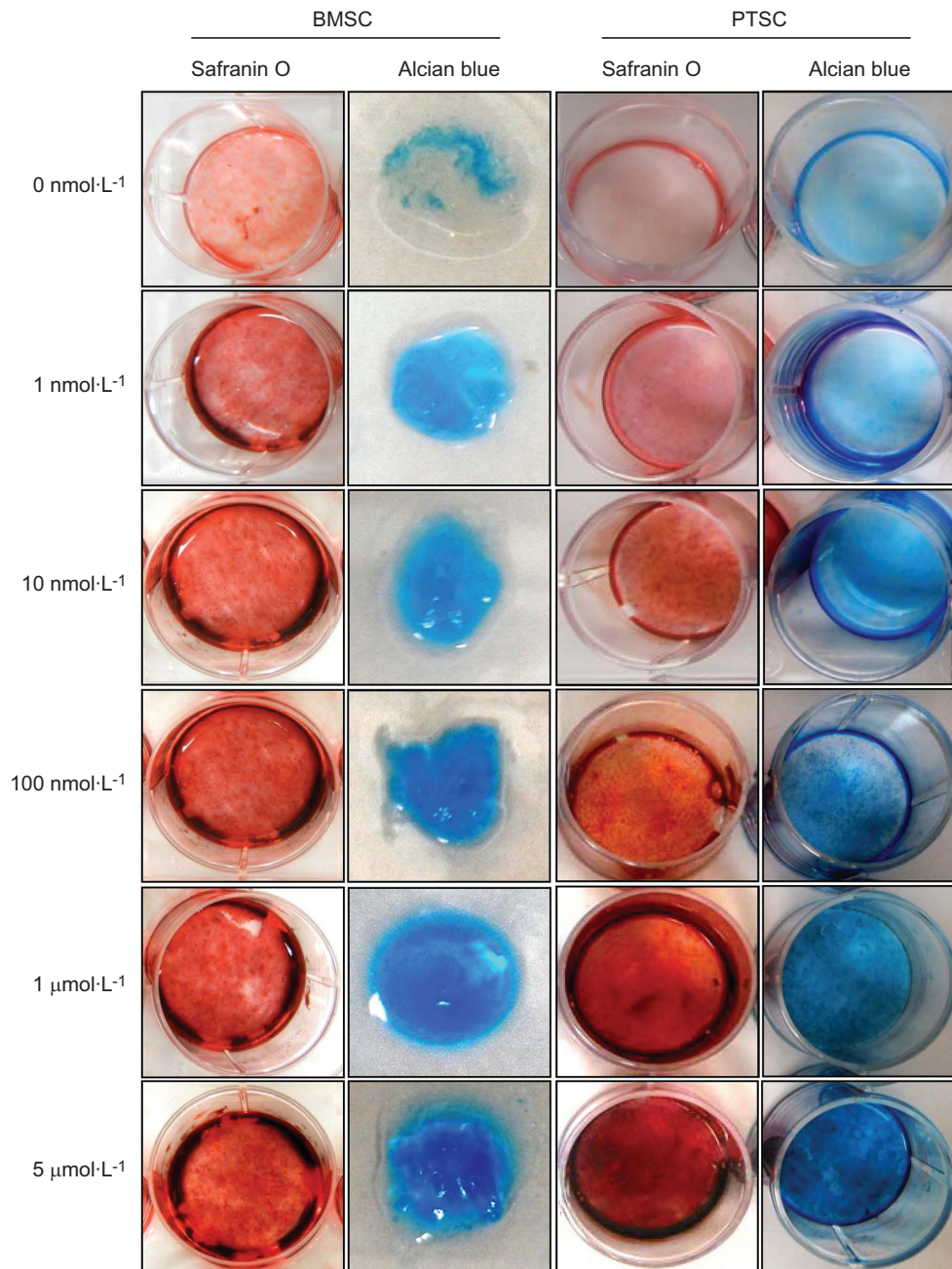


**Figure 3.** The effect of KGN on chondrogenic differentiation of rabbit BMSCs and PTSCs *in vitro*. BMSCs and PTSCs were cultured in medium containing KGN at concentrations ranging from  $1 \text{ nmol}\cdot\text{L}^{-1}$  to  $5 \text{ }\mu\text{mol}\cdot\text{L}^{-1}$  for 2 weeks and stained with Safranin O or Alcian blue. Cells without KGN treatment were used as a control ( $0 \text{ nmol}\cdot\text{L}^{-1}$ ). Staining for both Safranin O and Alcian blue increased with increasing levels of KGN in both cultures indicating that KGN increases chondrogenic differentiation of BMSCs and PTSCs.

higher with further increase in KGN levels (Figure 2a). Specifically, aggrecan levels in BMSCs treated with  $5 \text{ }\mu\text{mol}\cdot\text{L}^{-1}$  KGN reached the highest levels with an 8-fold increase over the non-treated control cells. Collagen II and Sox-9 mRNA levels stayed similar, with levels varying only slightly between them under all treatment conditions. Similar to aggrecan, both collagen II and Sox-9 gene expression levels also reached their maximum at  $5 \text{ }\mu\text{mol}\cdot\text{L}^{-1}$  KGN, with a 5-fold increase when compared

to the control cells without KGN treatment. On the other hand, the chondrogenic response of PTSCs to KGN treatment was different from BMSCs. While all three chondrogenic gene markers in PTSCs also increased in a dose-dependent manner, the maximum expression level observed for collagen II was a 31-fold increase over control cell levels (Figure 2b). Similarly, both aggrecan and Sox-9 mRNA levels also increased with increasing KGN concentrations in the medium, although their maximum

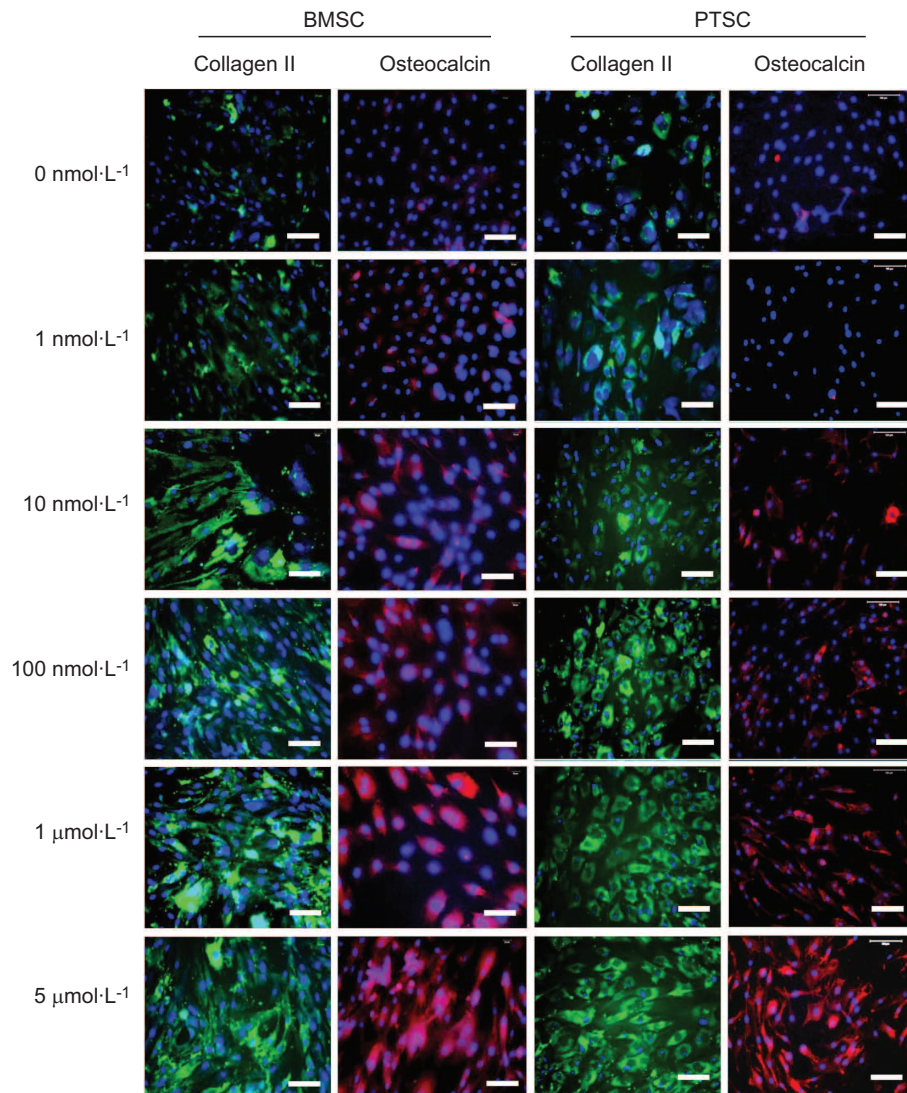


**Figure 4.** Chondrogenic differentiation of rabbit BMSCs and PTSCs cultured *in vitro* in medium containing KGN. BMSCs and PTSCs were grown in medium with various concentrations of KGN ( $1 \text{ nmol}\cdot\text{L}^{-1}$ – $5 \text{ }\mu\text{mol}\cdot\text{L}^{-1}$ ). The cells without KGN treatment were used as a control. After being treated for 2 weeks in culture, the cells were immunostained with anti-collagen II and anti-osteocalcin antibodies to determine chondrogenic differentiation. Nuclei were stained with Hoechst fluorochrome 33342 (blue). Chondrogenic differentiation in both cell types increased after the addition of KGN in a dose-dependent manner. Bars=100  $\mu\text{m}$ .

increase was only 12-fold for aggrecan and 8-fold for Sox-9 (Figure 2b).

Consistent with the gene expression results, cytochemical analyses to determine proteoglycan accumulation using Safranin O and Alcian blue staining revealed an increase in staining intensity in both BMSCs and PTSCs cultured *in vitro* (Figure 3), indicating higher accumulation of proteoglycans in both cell types treated with various concentrations of KGN. This increased staining intensity also correlated with the increasing doses of KGN, reflecting a dose-dependent effect on cell chondrogenesis.

Further, immunocytochemical analyses of BMSCs and PTSCs (Figure 4) treated with KGN showed a clear dose-dependent increase in both collagen II and osteocalcin

expression, with maximum expression levels at  $5 \text{ }\mu\text{mol}\cdot\text{L}^{-1}$  KGN.

#### Effects of KGN on tendinous tissues *in vivo*

To determine the *in vivo* effect of KGN, we first administered four injections of  $100 \text{ }\mu\text{mol}\cdot\text{L}^{-1}$  KGN into intact rat patellar tendons and analyzed the injected area 15 days after the treatment. KGN injections induced drastic changes in the patellar tendons; they were covered with a thin layer of connective tissue, with newly formed vessels apparent across the tissue and, as a result, the shining appearance in the saline injected control tendons (Figure 5a) were no longer visible (Figure 5b). These morphological changes in the patellar tendons were corroborated by histochemical

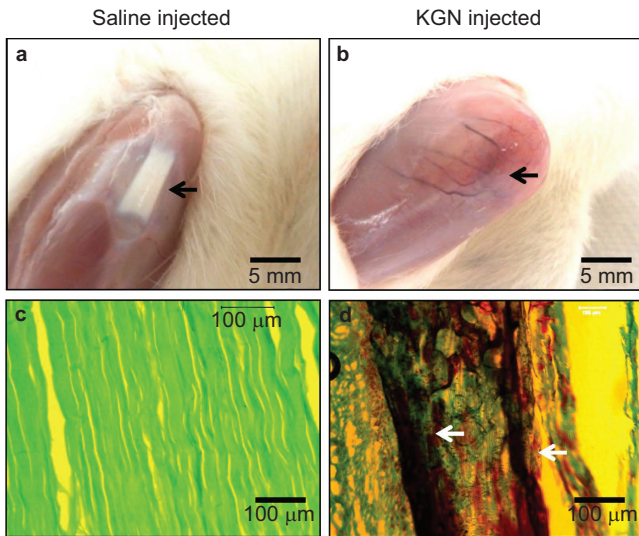


**Figure 5.** The effect of KGN injection on intact rat patellar tendons *in vivo*. Intact patellar tendons were injected with 10 μL saline (a, c) or 10 μL of 100 μmol·L<sup>-1</sup> KGN (b, d) four times, on days 1, 2, 7 and 14. Rats were then killed on day 15 to assess the effect of KGN on the patellar tendons. Intact tendons exhibit a white glistening appearance (a, arrow). However, after KGN injection, the original patellar tendon tissue is almost indistinguishable from the newly formed tissues, which appear highly vascularized (b). Staining of the corresponding tissue sections with fast green and Safranin O shows dense collagen in the saline-injected control (c), but extensive accumulation of proteoglycans (arrow) interspersed with collagen is observed in the KGN-injected patellar tendon (d).

staining, which showed intense staining for Safranin O in the KGN-treated patellar tissues (Figure 5d) and a lack of Safranin O staining in the control tendon injected with saline (Figure 5c) indicating the presence of abundant proteoglycan after KGN injections. While both control and KGN treated tendons were stained with fast green, which indicated the presence of collagen, staining in control tendons was much more extensive compared to the KGN-treated tendons, indicating the presence of large amounts of neo-proteoglycan due to KGN injections.

#### Effects of KGN on injured TBJs *in vivo*

In addition to injecting KGN into intact patellar tendons, we also determined the potential of KGN to enhance wound healing in a TBJ injury model. For this, intact rat Achilles tendons (Figure 6a) in the TBJs of the hind legs were punctured with a biopsy punch to create a wound or hole (Figure 6b). Injection of 100 μmol·L<sup>-1</sup> KGN indeed promoted healing of injured tissue after 15 days of treatment and appeared to form a more complete, mature and glistening cartilage-like tissue (Figure 6d); in contrast, the injured tissues injected with saline looked yellowish and healing appeared incomplete (Figure 6c). Histological analysis of these tissue sections stained with Safranin O showed that almost 90% of the KGN-injected tissue was stained positive (Figure 6f), compared to a lack of

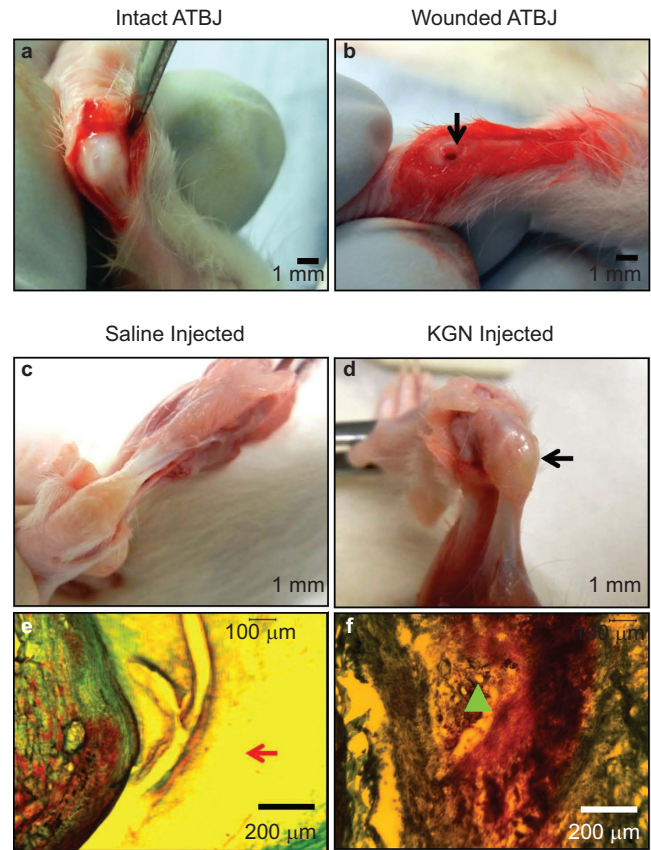


**Figure 6.** The effect of KGN injection on the healing of rat ATBJ. Intact Achilles tendon-bone junctions of rats were wounded (1 mm diameter) and then injected with 10 μL saline (c, e) or 10 μL of 100 μmol·L<sup>-1</sup> KGN four times, on days 1, 2, 7 and 14. The rats were killed on day 15 for examination. (a) Intact Achilles tendon-bone junction; (b) wounded ATBJ with a hole indicated by arrow; (c) natural healing of the wounded ATBJ 15 days after wounding; arrow indicates immature, yellowish cartilage-like tissue; (d) completely healed KGN-injected ATBJ 15 days after wounding; arrow points to large, glistening new cartilage-like tissue; (e) saline-injected wound site at the ATBJ stained with fast green and Safranin O shows the lack of proteoglycans in the wound area indicating the absence of fibrocartilage-like tissue formation in the junction; arrow points to the wounded ATBJ area that remained empty even after two weeks of healing. Bone tissues are visible on the left, while tendinous tissues stained with fast green are at the bottom right corner; (f) staining of the KGN-injected ATBJ wound with fast green and Safranin O shows formation of cartilage-like tissue; the wounded ATBJ appears to be filled with abundant proteoglycans stained with Safranin O (triangle), and tendinous tissues are located in the right and appear green with fast green staining. ATBJ, Achilles tendon-bone junction.

Safranin O positive staining in the saline-injected group (Figure 6e). Similar to the patellar tendon, fast green staining, indicating collagen, was intense only in the control (Figure 6e), but not in the KGN-treated area of the TBJ (Figure 6f).

#### DISCUSSION

Complete regeneration of TBJs after an injury continues to be a challenge in clinics. Indeed, healing at the tendon/

bone interface after ACL reconstruction surgeries has been accelerated by tissue engineering approaches, although limitations of using growth factors (MSCs, OMSCs, etc.) have been recognized. Our findings reported in this study show that the small drug-like molecule, KGN, stimulates cell proliferation, induces *in vitro* chondrogenic differentiation of two different adult stem cells, BMSCs and TSCs, and accelerates the formation of cartilage-like tissue within tendinous tissues and injured TBJ *in vivo*.

The normal TBJ is protected by a fibrocartilage transition zone which enables a gradual transition of mechanical property between tendon and bone, and as a result, decreases stress concentration, and enhances the strength of tissue bonding between tendon and bone. When the TBJ is injured, natural healing tends to be slow and does not completely restore the original strength of the TBJ. Therefore, surgical procedures have been adopted in clinical settings. However, thus far, surgical procedures alone have not been successful in regenerating the fibrocartilage zone in TBJs. Considering that KGN has a strong potential to induce chondrogenesis, as shown in this study, it may be a promising approach to apply KGN after reconstruction surgeries to promote healing, particularly healing of the fibrocartilage zone at the tendon/bone interface.

In clinics, tendon–bone healing is a particular challenge after ACL reconstruction, which is a common surgical procedure to re-create torn ACLs in injured knee joints to restore knee function.<sup>33–34</sup> To promote the healing of the tendon graft within the bone tunnel during ACL reconstruction, researchers have used hamstring tendon transfers,<sup>5,35–39</sup> tendon reattachment,<sup>40–41</sup> cytokine administration,<sup>14–15</sup> wrappings of periosteum<sup>20</sup> and hydroxyapatite<sup>42</sup> that anchors tendon to bone. All these approaches attempted to produce firm tendon–bone integration after ACL reconstruction surgeries. However, these approaches resulted in limited mechanical strength between the healed tendon and bone, because the fibrocartilage zone between the tendon graft and bone was often not established. Additionally, cell therapy approaches, such as implantation of MSCs, have been proposed to enhance healing of the tendon/bone interface,<sup>18,43–44</sup> but these approaches have downsides that make them less applicable in clinical settings.

In this study, we have shown that KGN could augment and accelerate the tendon/bone interface healing because of its potential to induce chondrogenic differentiation of stem cells, as evidenced by the intense staining for chondrogenic markers collagen II and osteocalcin (Figure 4) after KGN treatment. These findings indicate that KGN may be used to enhance tendon/bone interface healing through the direct, local delivery of KGN

injections into the gap between the tendon graft and the bone surface during ACL reconstruction. It is known that within a week after ACL reconstruction, a layer of fibrovascular tissue forms in the interface between the tendon graft and bone tunnel.<sup>23</sup> Therefore, KGN may be used after ACL reconstruction to specifically target the stem cells in the fibrovascular/connective tissues that are already present in the interface between the tendon graft and bone tunnel during the initial healing time. In other words, this KGN approach taps into mesenchymal regenerative cells to give rise to cartilage cells that form connective tissues. These regenerative cells include chondrocytes, the only cells in the body that produce cartilage; as shown in this study, KGN activates these cells to produce cartilage tissues. Therefore, we suggest that KGN treatment could be a cell-free therapy, which will be optimal to promote healing between bones and soft tissues.

In this study, we observed that the *in vitro* effect of KGN on BMSCs and PTSCs was dose-dependent. While low doses of KGN ( $10 \text{ nmol}\cdot\text{L}^{-1}$  and  $100 \text{ nmol}\cdot\text{L}^{-1}$ ) effectively induced chondrogenesis and osteogenesis in both BMSCs and PTSCs, higher KGN levels ( $1 \text{ }\mu\text{mol}\cdot\text{L}^{-1}$  and  $5 \text{ }\mu\text{mol}\cdot\text{L}^{-1}$ ) caused the formation of extensive cartilage-like tissues (Figure 4), which may be detrimental and deter healing of TBJ. Therefore, optimal doses should be determined based on tissue type, surgery type performed and patient history before attempting to use KGN for therapeutic use. Similar dose-dependent effects of KGN on the chondrogenic differentiation of human MSCs were also reported previously.<sup>27</sup> This study also reported that the potential systemic toxic effects of this compound *in vivo* at the tested concentration ( $100 \text{ }\mu\text{mol}\cdot\text{L}^{-1}$ ) was negligible, as evidenced by the low serum level of KGN absorbed from the intra-articular space,<sup>27</sup> which is an advantage of using KGN as a cell-free therapy.

It should be noted that this study was designed to test the feasibility of using KGN to induce chondrogenesis of stem cells and thereby enhance the healing of the tendon/bone interface. However, studies of longer term use (such as >26 weeks) and the effects of lesser amounts of KGN (such as one or two injections) are required to demonstrate whether the use of KGN injections can regenerate the fibrocartilage zone in injured TBJs, a key factor for the successful restoration of the TBJ structure and function. Moreover, the mode of KGN delivery to wounds in TBJs, in this case injection, may not be optimal; without a scaffold to control its movement, KGN cannot be guaranteed to be confined to the wound area and act in the intended location. This may be a problem because of KGNs' ability to form excessive cartilage-like tissues in unintended areas. For example, in our results (Figure 5b), the patellar tendon was no longer visible due to over growth of patellar tissues and surrounding tissues.



Therefore, KGN should be used with a bioscaffold, such as platelet-rich plasma, to form a matrix in the injected area and prevent KGN spreading into neighboring areas.<sup>45</sup> Platelet-rich plasma is a good choice for a bioscaffold, because the abundant growth factors it contains also stimulate the healing of injured tissues. In addition, for ACL reconstructions, KGN could be used along with engineered tendon matrix<sup>46</sup> to enhance tendon graft-bone tunnel healing and promote the formation of fibrocartilage regeneration in the interface. Use of engineered tendon matrix serves a dual purpose: on the one hand, engineered tendon matrix contains the mature matrix that stem cells need to proliferate and differentiation into tenocytes, which in turn would repair injured tendons in the TBJ; on the other hand, KGN itself could stimulate stem cells to undergo chondrogenic differentiation that would enhance the formation of the fibrocartilage zone, which could improve the healing speed and quality of tendon/bone interface.

## CONCLUSIONS

Regeneration of the TBJ after an injury is a significant challenge in clinics. This study showed that use of a small molecule called KGN could be a promising approach to augment and accelerate the formation of cartilage-like tissue in the tendon/bone interface in the TBJ as well as in ACL reconstruction. Compared to many tissue engineering approaches used in tendon/bone interface healing, KGN may be easier to apply in clinical settings as a convenient, cell-free therapy. Future research is required to determine optimal KGN dosage regimens and to evaluate the effects of KGN-scaffold composites on tendon/bone interface healing.

## Conflict of Interest

The authors declare that they have no competing interests.

## Acknowledgements

The funding support from NIH/NIAMS (AR061395, AR060920, and AR049921) for this work is gratefully acknowledged (JHW). We thank Dr Dapeng Jian for his assistance in performing KGN injection experiments and Dr Nirmala Xavier for assistance in preparing the manuscript.

## References

- 1 Benjamin M, Toumi H, Ralphs JR, Bydder G, Best TM, Milz S. Where tendons and ligaments meet bone: attachment sites ('entheses') in relation to exercise and/or mechanical load. *J Anat* 2006; **208**: 471–490.
- 2 Hibino N, Hamada Y, Sairyo K, Yukata K, Sano T, Yasui N. Callus formation during healing of the repaired tendon-bone junction. A rat experimental model. *J Bone Joint Surg Br* 2007; **89**: 1539–1544.
- 3 Raspanti M, Stocchi R, de Pasquale V, Martini D, Montanari C, Ruggeri A. Structure and ultrastructure of the bone/ligament junction. *Ital J Anat Embryol* 1996; **101**: 97–105.
- 4 Woo S, Manynard J, Butler D. Ligament, tendon, and joint capsule insertions to bone. In: Woo S, Buckwalter J (ed.), *Injury and Repair of the Musculoskeletal Soft Tissues*. Park Ridge, IL: American Academy of Orthopaedic Surgeons Symposium, 1988: 129–166.
- 5 Nebelung W, Becker R, Urbach D, Ropke M, Roessner A. Histological findings of tendon-bone healing following anterior cruciate ligament reconstruction with hamstring grafts. *Arch Orthop Trauma Surg* 2003; **123**: 158–163.
- 6 Leung K, Qin L, Fu L, Chan C. Bone to bone repair is superior to bone to tendon healing in patella-patellar tendon complex – an experimental study in rabbits. *J Clin Biomech* 2002; **17**: 594–602.
- 7 Liu S, Hang D, Gentili A, Finerman G. MRI and morphology of the insertion of the PT after graft harvesting. *J Bone Joint Surg (Br)* 1996; **78**: 823–826.
- 8 Wong M, Qin L, Lee K *et al*. Healing of bone-tendon junction in a bone trough: A goat partial patellectomy model. *Clin Orthop* 2003; **413**: 291–302.
- 9 Galatz LM, Sandell LJ, Rothermich SY *et al*. Characteristics of the rat supraspinatus tendon during tendon-to-bone healing after acute injury. *J Orthop Res* 2006; **24**: 541–550.
- 10 Oguma H, Murakami G, Takahashi-Iwanaga H, Aoki M, Ishii S. Early anchoring collagen fibers at the bone-tendon interface are conducted by woven bone formation: light microscope and scanning electron microscope observation using a canine model. *J Orthop Res* 2001; **19**: 873–880.
- 11 Qin L, Leung K, Chan C, Fu L, Rosier R. Enlargement of remaining patella after partial patellectomy in rabbits. *Med Sci Sports Exerc* 1999; **314**: 502–506.
- 12 Anderson K, Seneviratne AM, Izawa K, Atkinson BL, Potter HG, Rodeo SA. Augmentation of tendon healing in an intraarticular bone tunnel with use of a bone growth factor. *Am J Sports Med* 2001; **29**: 689–698.
- 13 Martinek V, Latterman C, Usas A *et al*. Enhancement of tendon-bone integration of anterior cruciate ligament grafts with bone morphogenetic protein-2 gene transfer: a histological and biomechanical study. *J Bone Joint Surg Am* 2002; **84-A**: 1123–1131.
- 14 Rodeo SA, Suzuki K, Deng XH, Wozney J, Warren RF. Use of recombinant human bone morphogenetic protein-2 to enhance tendon healing in a bone tunnel. *Am J Sports Med* 1999; **27**: 476–488.
- 15 Yamazaki S, Yasuda K, Tomita F, Tohyama H, Minami A. The effect of transforming growth factor-beta1 on intraosseous healing of flexor tendon autograft replacement of anterior cruciate ligament in dogs. *Arthroscopy* 2005; **21**: 1034–1041.
- 16 Yoshikawa T, Tohyama H, Katsura T *et al*. Effects of local administration of vascular endothelial growth factor on mechanical characteristics of the semitendinosus tendon graft after anterior cruciate ligament reconstruction in sheep. *Am J Sports Med* 2006; **34**: 1918–1925.
- 17 Weiler A, Forster C, Hunt P *et al*. The influence of locally applied platelet-derived growth factor-BB on free tendon graft remodeling after anterior cruciate ligament reconstruction. *Am J Sports Med* 2004; **32**: 881–891.
- 18 Lim JK, Hui J, Li L, Thambyah A, Goh J, Lee EH. Enhancement of tendon graft osteointegration using mesenchymal stem cells in a rabbit model of anterior cruciate ligament reconstruction. *Arthroscopy* 2004; **20**: 899–910.
- 19 Nourissat G, Diop A, Maurel N *et al*. Mesenchymal stem cell therapy regenerates the native bone-tendon junction after surgical repair in a degenerative rat model. *PLoS ONE* 2010; **5**: e12248.
- 20 Kyung HS, Kim SY, Oh CW, Kim SJ. Tendon-to-bone tunnel healing in a rabbit model: the effect of periosteum augmentation at the tendon-to-bone interface. *Knee Surg Sports Traumatol Arthrosc* 2003; **11**: 9–15.
- 21 Youn I, Jones DG, Andrews PJ, Cook MP, Suh JK. Periosteal augmentation of a tendon graft improves tendon healing in the bone tunnel. *Clin Orthop Relat Res* 2004; **419**: 223–231.
- 22 Chen CH, Chen WJ, Shih CH, Yang CY, Liu SJ, Lin PY. Enveloping the tendon graft with periosteum to enhance tendon-bone healing in a bone

- tunnel: a biomechanical and histologic study in rabbits. *Arthroscopy* 2003; **19**: 290–296.
- 23 Hays PL, Kawamura S, Deng XH *et al.* The role of macrophages in early healing of a tendon graft in a bone tunnel. *J Bone Joint Surg* 2008; **90**: 565–579.
- 24 Inagaki Y, Uematsu K, Akahane M *et al.* Osteogenic matrix cell sheet transplantation enhances early tendon graft to bone tunnel healing in rabbits. *Biomed Res Int* 2013; **2013**: 842192.
- 25 Dickerson DA, Misk TN, van Sickle DC, Breur GJ, Nauman EA. *In vitro* and *in vivo* evaluation of orthopedic interface repair using a tissue scaffold with a continuous hard tissue-soft tissue transition. *J Orthop Surg Res* 2013; **8**: 18–28.
- 26 Schönmeier B, Clavin N, Avraham T, Longo V, Mehrara BJ. Synthesis of a tissue-engineered periosteum with acellular dermal matrix and cultured mesenchymal stem cells. *Tissue Eng Part A* 2009; **15**: 1833–1841.
- 27 Johnson K, Zhu S, Tremblay MS *et al.* A stem cell-based approach to cartilage repair. *Science* 2012; **336**: 717–721.
- 28 Gnechi M, Melo LG. Bone marrow-derived mesenchymal stem cells: isolation, expansion, characterization, viral transduction, and production of conditioned medium. *Methods Mol Biol* 2009; **482**: 281–294.
- 29 Zhang J, Wang JH. Characterization of differential properties of rabbit tendon stem cells and tenocytes. *BMC Musculoskelet Disord* 2010; **11**: 10–20.
- 30 Emans PJ, Spaapen F, Surtel DA *et al.* A novel *in vivo* model to study endochondral bone formation; HIF-1 $\alpha$  activation and BMP expression. *Bone* 2007; **40**: 409–418.
- 31 Majima T, Marchuk LL, Sciore P, Shrive NG, Frank CB, Hart DA. Compressive compared with tensile loading of medial collateral ligament scar *in vitro* uniquely influences mRNA levels for aggrecan, collagen type II, and collagenase. *J Orthop Res* 2005; **18**: 524–531.
- 32 Yang Y, Zhang J, Qian Y *et al.* Superparamagnetic iron oxide is suitable to label tendon stem cells and track them *in vivo* with MR imaging. *Ann Biomed Eng* 2013; **41**: 2109–2119.
- 33 Fabricant PD, Jones KJ, Delos D *et al.* Reconstruction of the anterior cruciate ligament in the skeletally immature athlete: a review of current concepts: AAOS exhibit selection. *J Bone Joint Surg Am* 2013; **95**: e28.
- 34 Chambat P, Guier C, Sonnery-Cottet B, Fayard JM, Thaunat M. The evolution of ACL reconstruction over the last fifty years. *Int Orthop* 2013; **37**: 181–186.
- 35 Robert H, Es-Sayeh J, Heymann D, Passuti N, Eloit S, Vaneenoge E. Hamstring insertion site healing after anterior cruciate ligament reconstruction in patients with symptomatic hardware or repeat rupture: a histologic study in 12 patients. *Arthroscopy* 2003; **19**: 948–954.
- 36 Weiler A, Hoffmann RF, Bail HJ, Rehm O, Sudkamp NP. Tendon healing in a bone tunnel. Part II: Histologic analysis after biodegradable interference fit fixation in a model of anterior cruciate ligament reconstruction in sheep. *Arthroscopy* 2002; **18**: 124–135.
- 37 Yoshiya S, Nagano M, Kurosaka M, Muratsu H, Mizuno K. Graft healing in the bone tunnel in anterior cruciate ligament reconstruction. *Clin Orthop Relat Res* 2000; **376**: 278–286.
- 38 Goradia VK, Rochat MC, Grana WA, Rohrer MD, Prasad HS. Tendon-to-bone healing of a semitendinosus tendon autograft used for ACL reconstruction in a sheep model. *Am J Knee Surg* 2000; **13**: 143–151.
- 39 Grana WA, Egle DM, Mahnken R, Goodhart CW. An analysis of autograft fixation after anterior cruciate ligament reconstruction in a rabbit model. *Am J Sports Med* 1994; **22**: 344–351.
- 40 Uthoff HK, Sano H, Trudel G, Ishii H. Early reactions after reimplantation of the tendon of supraspinatus into bone. A study in rabbits. *J Bone Joint Surg Br* 2000; **82**: 1072–1076.
- 41 Boyer MI, Harwood F, Ditsios K, Amiel D, Gelberman RH, Silva MJ. Two-portal repair of canine flexor tendon insertion site injuries: histologic and immunohistochemical characterization of healing during the early postoperative period. *J Hand Surg Am* 2003; **28**: 469–474.
- 42 Ishikawa H, Koshino T, Takeuchi R, Saito T. Effects of collagen gel mixed with hydroxyapatite powder on interface between newly formed bone and grafted achilles tendon in rabbit femoral bone tunnel. *Biomaterials* 2001; **22**: 1689–1694.
- 43 Haleem AM, Singergy AA, Sabry D *et al.* The clinical use of human culture-expanded autologous bone marrow mesenchymal stem cells transplanted on platelet-rich fibrin glue in the treatment of articular cartilage defects: a pilot study and preliminary results. *Cartilage* 2010; **1**: 253–261.
- 44 Ju YJ, Muneta T, Yoshimura H, Koga H, Sekiya I. Synovial mesenchymal stem cells accelerate early remodeling of tendon–bone healing. *Cell Tissue Res* 2008; **332**: 469–478.
- 45 Zhang J, Middleton KK, Fu FH, Im HJ, Wang JH. HGF mediates the anti-inflammatory effects of PRP on injured tendons. *PLoS ONE* 2013; **8**: e67303.
- 46 Zhang J, Li B, Wang JH. The role of engineered tendon matrix in the stemness of tendon stem cells *in vitro* and the promotion of tendon-like tissue formation *in vivo*. *Biomaterials* 2011; **32**: 6972–6981.



This work is licensed under a Creative Commons Attribution-NonCommercial-NoDerivs 3.0 Unported License. The images or other third party material in this article are included in the article's Creative Commons license, unless indicated otherwise in the credit line; if the material is not included under the Creative Commons license, users will need to obtain permission from the license holder to reproduce the material. To view a copy of this license, visit <http://creativecommons.org/licenses/by-nc-nd/3.0/>